Seismic exploration equipment: set-up and survey test

Author: Marc Gener Milán.
*Facultat de Física, Universitat de Barcelona, Diagonal 645, 08028 Barcelona, Spain.**

Advisor: Pilar Queralt Capdevila

Abstract: Seismic Refraction Tomography (SRT) is a common geophysical technique used to obtain the mechanical properties of a terrain from the study of near-surface propagation velocity of elastic waves. In this work we make a test survey to setup a SRT equipment and ensure that it is ready for use. We also evaluate a new data-analysis software and conclude with some usage recommendations.

I. INTRODUCTION

Proper setup and preparation are crucial to the success of any experimental work. These first steps, which include checking for instrument malfunctions, anticipating to possible challenges or familiarising with new (never-used-before) equipment or software, usually pay off later in terms of time, effort and even economic savings and are essential to gather good quality data.

We will put this into practise with a new equipment, a compact unit by the german company DMT [1], acquired by our university, and a new open-source software [2] in a Seismic Refraction Tomography (SRT) survey.

SRT is an active method that consists in generating elastic waves on the surface of the site of study that are refracted as they propagate underground through different materials. Part of these waves come back to the surface where they are detected and registered for later analysis. This allows us to characterise the ground materials and infer their in-depth distribution and wave propagation velocity. The fundamentals of this technique are detailed in the next section following the explanation in Chapter 6 of Mark E. Everett [3].

The main objectives are to successfuly setup the equipment and software so that it is ready to use, and to give some recommendations for future users based in our experience and test results.

II. THEORETICAL BACKGROUND

A. Elastic waves

The main magnitudes used to describe elastic materials are stress and strain.

The stress tensor σ quantifies the force per unit area $[N/m^2 \; or \; Pa]$ exerted over the elastic body. If the force is perpendicular to the body's surface it is called a pressure, responsible of dilations and contractions (volume changes). If the force is parallel to the surface then it's called shear stress, responsible of changes in shape.

On the other hand, strains ε are the measure of the deformation of a body under some kind of stress. The strain is a dimensionless quantity.

We can define the dilatation of a body Δ, as:

$$\Delta = \sum_i \varepsilon_{ii} = \varepsilon_{xx} + \varepsilon_{yy} + \varepsilon_{zz}. \tag{1}$$

Taking an ideal case where strains are small, which applies to near-surface seismology, the relation between stress and strain follows Hooke's law

$$\begin{gathered} \sigma_{ii} = \lambda\Delta + 2\mu\varepsilon_{ii} \quad for \quad i = x, y, z \\ \sigma_{ij} = \mu\varepsilon_{ij} \quad for \quad i \neq j \end{gathered} \tag{2}$$

where $\lambda > 0, \mu$ are the Lamé parameters which have the same units as stress $[N/m^2 \; or \; Pa]$.

Now let's consider the motion that unbalanced stresses cause on elastic materials. Rewriting Newton's formula $\vec{F} = m\vec{a}$ in an infinitessimal version for the displacement along the x component

$$\rho \frac{\partial^2 u_x}{\partial t^2} = \frac{\partial \sigma_{xx}}{\partial x} + \frac{\partial \sigma_{xy}}{\partial y} + \frac{\partial \sigma_{xz}}{\partial z} \tag{3}$$

and using Eq. (1) and (2) we get that

$$\rho \frac{\partial^2 u_x}{\partial t^2} = (\lambda + \mu)\frac{\partial \Delta}{\partial x} + \mu\nabla^2 u_x, \tag{4}$$

where ∇^2 is the Laplacian operator. Equations (3) and (4) also stand for y and z displacements.

Finally, differentiating each equation of the type (4) with respect to their corresponding coordinate (x,y or z) and adding them up, results in

$$\rho \frac{\partial^2 \Delta}{\partial t^2} = (\lambda + 2\mu)\nabla^2 \Delta. \tag{5}$$

Renaming the terms we get to the well known wave equation

$$\frac{1}{V_P^2}\frac{\partial^2 \Delta}{\partial t^2} = \nabla^2 \Delta \tag{6}$$

with $V_P = \sqrt{(\lambda + 2\mu)/\rho}$.

*Electronic address: mgenermi7@alumnes.ub.edu

This describes the compressional waves (P-waves) in an elastic material with propagation velocity V_P. An analogous result can be obtained for the rotational parameter $\theta_x = \partial u_z/\partial y - \partial u_y/\partial z$ (also for θ_y and θ_z)

$$\frac{1}{V_S^2}\frac{\partial^2\theta_x}{\partial t^2} = \nabla^2\theta_x \tag{7}$$

with $V_S = \sqrt{\mu/\rho}$. This describes the shear waves (S-waves) in an elastic material with propagation velocity V_S which is, in general, lower than V_P for solid materials. Thus we conclude it is possible to apply the known wave propagation theory to elastic waves.

B. Wave propagation

Suppose a simple model of the near sub-surface with two layers of different materials (FIG 1). When an incident wave encounters the medium change, it follows the widely known reflection and refraction laws

$$\theta_i = \theta_r \quad ; \quad \frac{sin(\theta_i)}{V_1} = \frac{sin(\theta_t)}{V_2} \tag{8}$$

where V_1 and V_2 are the velocities [m/s] of the wave in each material layer; $\theta_i, \theta_r, \theta_t$ are the angles of the incident, the reflected and the refracted ray respectively.

At Eq. (8) we see it is possible to get a refracted wave at $\theta_t = 90°$ if $V_1 < V_2$. This is called the critically refracted ray.

A detector located at a certain distance from the source of the elastic waves, will register the direct, the reflected and the critically refracted waves, each at different arrival times.

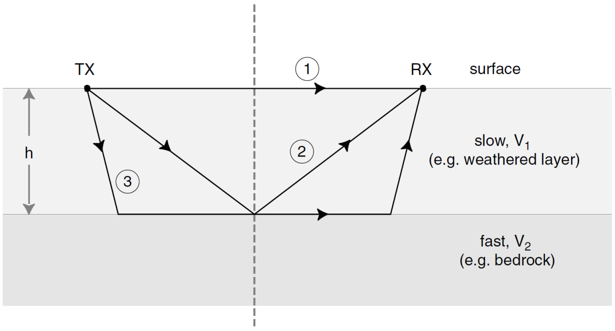

FIG. 1: Scheme of a 2-layered model with the trajectory of the direct (1), reflected (2), and critically refracted (3) rays from the source of the wave (TX) to the receiver (RX). Extracted from [3].

After some simple calculations, we can see that only the direct and the refracted waves will ever be a first arrival. Their travel-time equations are

$$t(x) = x/V_1 \quad Direct \tag{9}$$

$$t(x) = \frac{x}{V_2} + \frac{2h\sqrt{V_2^2 - V_1^2}}{V_1 V_2} \quad Refracted \tag{10}$$

where t [s] is the time of arrival, x [m] the distance from the source to the receiver. These equations describe straight lines in the t-x diagram. (FIG 2)

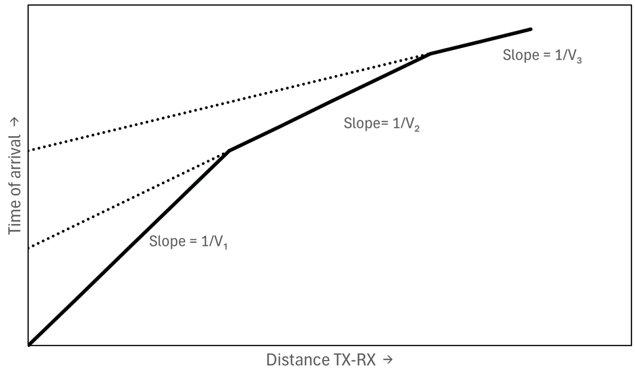

FIG. 2: t-x diagram extended to a 3-layer model.

The point where the direct and refracted time travel lines cross is called the crossover distance

$$x_C = 2h\frac{\sqrt{V_2 + V_1}}{\sqrt{V_2 - V_1}} \tag{11}$$

For $x > x_C$ the refracted rays are the first arrivals.

C. Picking

Picking is the process of selecting the first arrival of the elastic waves to each geophone, and the main step of the whole campaign. In fact, it is the proper data acquisition phase, because we will not use the whole geophone registers for the analysis, only the first arrival times of the seismic waves.

Picking usually is a hand-made process. Even when a program is used for a fast automated picking, then it is later manually revised to ensure it is accurate. It requires experience, neat data and help from a specialised software to make the most precise of pickings.

D. Inversion

The inversion process consists of an iterative method to obtain a possible sub-surface model compatible with the experimental data we have. This is done by specialised software which may offer more than one algorithm to work with. These methods are described in the program's manuals.

The general approach is the following: The first arrivals picked are the input data. The program starts with a pre-defined simple model of the sub-surface, discretised in different propagation velocity sections, and calculates the ray tracing following this model (This step is called solving the "direct problem"). The result obtained is compared to our input data, and the model is changed according to the calculated discrepancies. Finally, the new model is used to start the process again until the error between the result of the direct problem and the data is low enough. Then the program outputs the last model computed. A more detailed description of the algorithm is not needed as it is not in the scope of our work.

For simplicity, we will use each program's default settings.

III. EQUIPMENT DESCRIPTION

A. Field equipment

The fundamental field equipment comprises the main DMT Summit System Instrument [1], the receivers and the wave source.

The core is a central compact unit which controls the register process and sends that information to the PC. It is connected using a 24 channel cable to the detectors. Each of them has a channel assigned by the compact unit, and can be numbered at convenience by the user. The compact unit has space for 2 cables of 24 channels.

Our receivers are 24 P-type and 5 S-type electromagnetic seismometers (or geophones, FIG. Appx.1). These are made of an external housing with a spike (or two for S-type geophones) and a head. The spike part is used to pin the receiver into the ground, so that it vibrates in solidarity with it. The head part contains a coil and a magnet, one fixed to the housing and the other suspended by a spring. When the elastic wave arrives, the geophone shakes, and the relative movement of the magnet and the coil induces a voltage. This signal is processed and sent to the PC to show the seismogram registered.

The source of the waves is a 6 Kg sledgehammer that will impact on a metal plate placed on the ground. For each hit, we register a data "shot".

A trigger system is also needed to command the equipment when to start the data gathering. The sledgehammer and the metal plate are each connected by a cable to the USB Line Interface, which is the bridge between the compact unit and the PC. The compact unit is constantly registering, but when there is a hit with the hammer, the trigger circuit closes and the computer selects which part of the register has to be saved, depending on the parameters previously set by the user.

To power the equipment, we used 12 V car batteries and a transformer to charge the computer.

It is also recommended, for ergonomy reasons, to bring a portable table and stools to work with the PC, as it is important to check the register obtained before saving. Most of the equipment is shown in Fig Appx.2

B. Software

PyRefra is a Python-based open-source software recently published by Hermann Zeyen and Emmanuel Léger for refraction seismic data treatment [2]. It includes many interesting functions, and it takes advantage of some previously developed packages for geophysical analysis or general scientific purposes. For us, its importance resides in the fact that it is an academy-oriented program. Interface shown in FIG. Appx.3

ZondST2D is a commercial software designed to visualise and process data from seismic tomography [4]. It is a program that, among many other functions, allows us to do the picking and the inversion in a simple way.

As it is a program we have used before in the Geophysics lectures, we will use it as a reference to check that the new program works as intended, but we will not use it for the data analysis. We will also compare the user experience of using both softwares.

Note that we used the demo version of this program.

IV. FIELD REPORTS

A. Day 1: Biology gardens 06/03/24

For the first day we registered a well-known terrain, the garden near the biology faculty, where, for some years, the geophysics course students have tested the SRT.

We prepared the acquisition program to be ready for measurement, following the manual's instructions to set the desired parameters. First of all, we checked that all geophones were detected by the computer so that none of them nor their connection to the compact unit was malfunctioning. The first attempt was not successful, as none of the receivers was detected as available. After a system restart the problem was solved.

In second place, we performed a geophone check, which is an option that allows us to characterise our geophones with several parameters. This was important because we used two receivers of unknown properties that were lend to us. The main parameter of the geophones is their natural frequency, and, with the check, we can state that all of them have the same one, 10 Hz. There was also a measure of noise, Impedance, and other magnitudes that may be useful in another context. FIG. Appx.4

We could now proceed to the recording. For this first day we did a simple register to confirm that the compact unit and the receivers were working.

B. Day 2: Esports UB field 11/04/24

The second day, we moved our site to the University Sports facilities. Over there is an unused field where, some years ago, a prospection was made. This way, we know what to expect from the analysis.

When we were placing the receivers, we noted that the surface soil was much dryer than the biology one, and full of little stones, so it was impossible to install some of them. That's why we had to dig a little hole, allowing us to place them, but less tightened to the ground as they should be, as it may affect the received signal.

To get a better survey than the first day, we placed the geophones 2m apart instead of 1m and then we repeated the same shots with the geophones displaced 1m forward. In this way, we were able to obtain a register as if we had 48 receivers. We took a shot every 2m starting from position of the first receiver before displacement.

When we finished, we made a small test with S-type geophones, and a metal bar half-buried into the ground to produce the waves but resulted unsuccessful. This was due to the bad coupling of the S geophones with the ground and also an inappropriate experimental design, as , with the setup used, we were generating mixed P and SV (vertical) waves called "Rayleigh" waves. Then the p arrival masks the S signal.

C. Day 3: Biology gardens 07/05/24

We repeated the same line as in day 1 but tried several features to explore their helpfulness. First, we included a pre-trigger time to the saved data, this means a time before the trigger was activated is also recorded.

In second place we added a gain (amplification) to the registered signal, but it didn't make such a difference at first sight. It can be applied later in the data analysis.

Then, we took some measures with stacking. This function sums the signal of more than one wave generated. This way we can magnify the efect of the signal we want, as white noise cancels out, but, in an urban environment, noise singals are also amplified (e.g.the metro passing by).

At last, we also retried the S-wave test with a better design than on day 2. We folded half a line so that on one side we had six P-type geophones and, on the other side, the five S-type geophones we have and a final P-type geophone to fill the line. In this way, we registered the arrivals of the P and S (Love, pure SH) waves to measure their speed difference. The difference is the placement of the metal bar, perpendicular to the line, to generate "Love", almost pure SH, waves.

V. DATA ANALYSIS

We detected some major errors in many of the shots registered. As an example, observe FIG. 3.

The first arrival for the geophone closest to the source (Offset=0 m) has been lost due to delay in the acquisition. This has happened to many of our shots We also observe a stair-like pattern in the first arrivals because of the difference in delay for different hammer hits.

As it is impossible to avoid errors or noise, it is crucial to have a program that takes into account a measuring error in its inversion calculations.

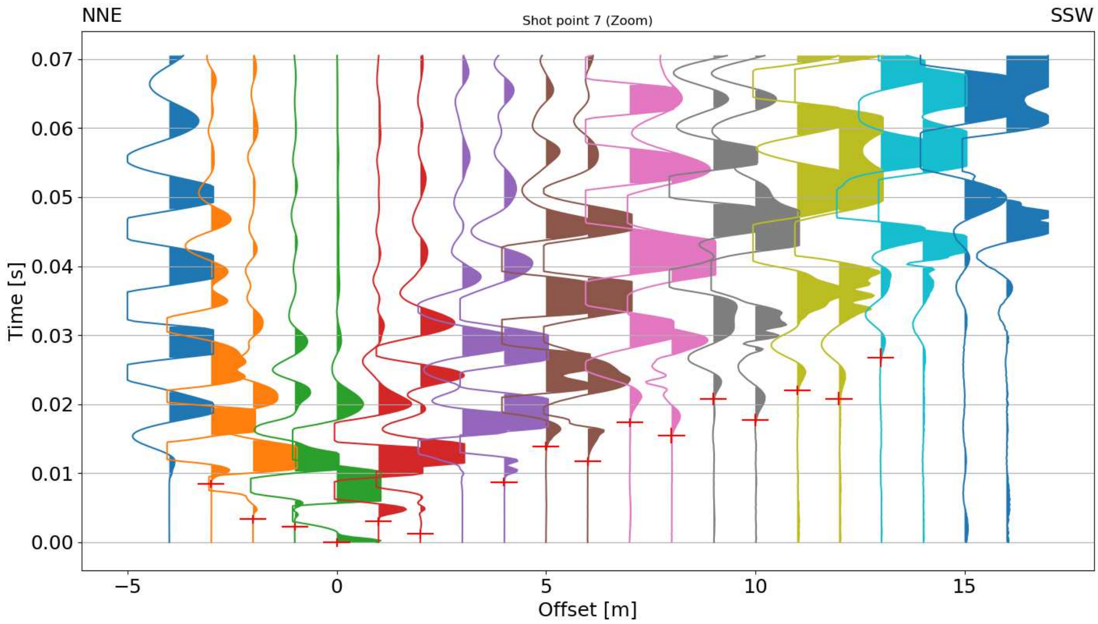

FIG. 3: Zoomed image showing errors encountered on shot 7.

PyRefra allows the user to introduce a manual error for each picked point (vertical line of the red crosses in FIG. 3 and Appx.3).

Using these registers from day 2, and despite our data not being of the best quality, we have been able to get a reasonable final model, in 21 iterations and with a $chi^2 = 2.6$, shown in FIG. 4.

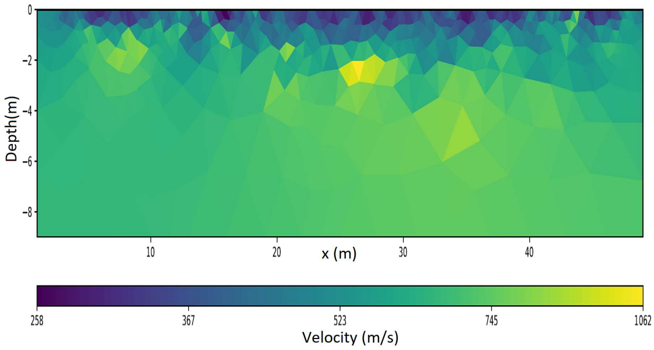

FIG. 4: Velocity profile model resulting from the inversion

As we expected, the terrain is composed of low velocity materials, mostly in the range of 400-800 m/s, and there is not a major anomaly in the terrain.

A more complete version of the results are shown in FIG. Appx.5

As a last analysis, let's see the comparison between P and S waves velocities we tested on day 3.

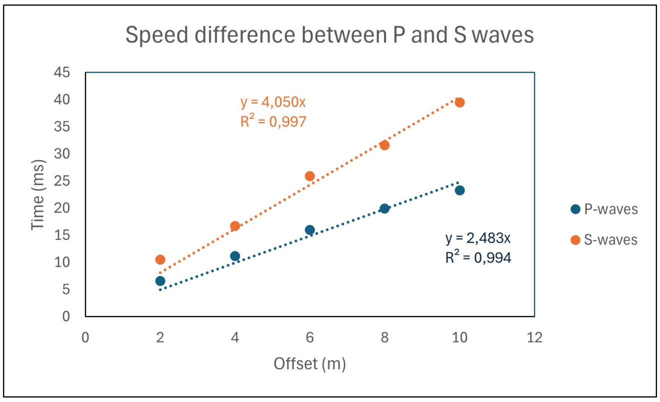

FIG. 5: First arrival times picked from simultaneous P and S geophones registers

As the velocity is the inverse of the slope, we get that

$$V_P \approx 400\ m/s \quad V_S \approx 250\ m/s$$

Which is compatible with our model and with the fact that, for most ground materials, V_S is usually between 40%-60% of V_P.

VI. CONCLUSIONS

First of all, we can ensure that the setup was successful and both the new equipment and software are checked and ready for a survey.

Based on the results obtained and challenges encountered, our recommendations to future users are:

Make sure that your equipment is complete and functional. Take your time to prepare the campaign. We recommend having a checklist to not forget any material and also bringing, some backup equipment and repair kit for any inconvenience.

It is highly recommended to set a pre-trigger time to avoid losing data due to computer registering delay. We have seen that a 25 ms pre-trigger time is more than enough to avoid loosing information. Both programs allow to later set t=0 to the correct time.

A propper survey design, combining P and S geophones, granted us enough resolution to obtain a value for V_S, which is not a simple task.

Using an open-source program made from an academic point of view improves both the understanding of the job done and the quality-of-life during the data treatment phase of the project. It also encourages a positive-feedback loop between the user and the programmer. Nonetheless, it is a non-trivial task to install the PyRefra software and to learn how to conveiniently input the information of the geometry and the shot positions. A further insight on the use of the program is given in the section **C** of the Appendix.

Acknowledgments

A huge thanks to Hermann Zeyen and David Garcia for their help and mostly to my advisor, Pilar Queralt, for her guidance and patience.

[1] DMT, *Summit System Instrument Help : Your Seismic Acquisition System for More Flexibility*, Version 1.4

[2] Hermann Zeyen, Emmanuel Léger, "PyRefra - Refraction seismic data treatment and inversion". Computers & Geosciences **185**, 2024

[3] Mark E. Everett, *Near-surface applied geophysics*, 1st. ed. (Cambridge University Press, New York, 2013)

[4] ZondST2D (2001-2018), User manual, *Program for processing and two-dimensional interpretation of seismic tomography data (land, borehole and marine surveys)*, Version 4.3 (Demo), Zond geophysical software.

VII. APPENDIX

A. Insrtumentation

FIG. Appx.1: Image of a P-geophone, of natural frequency 10 Hz, (left); and an S-geophone, of natural frequency 5 Hz, (right) that we used in our survey.

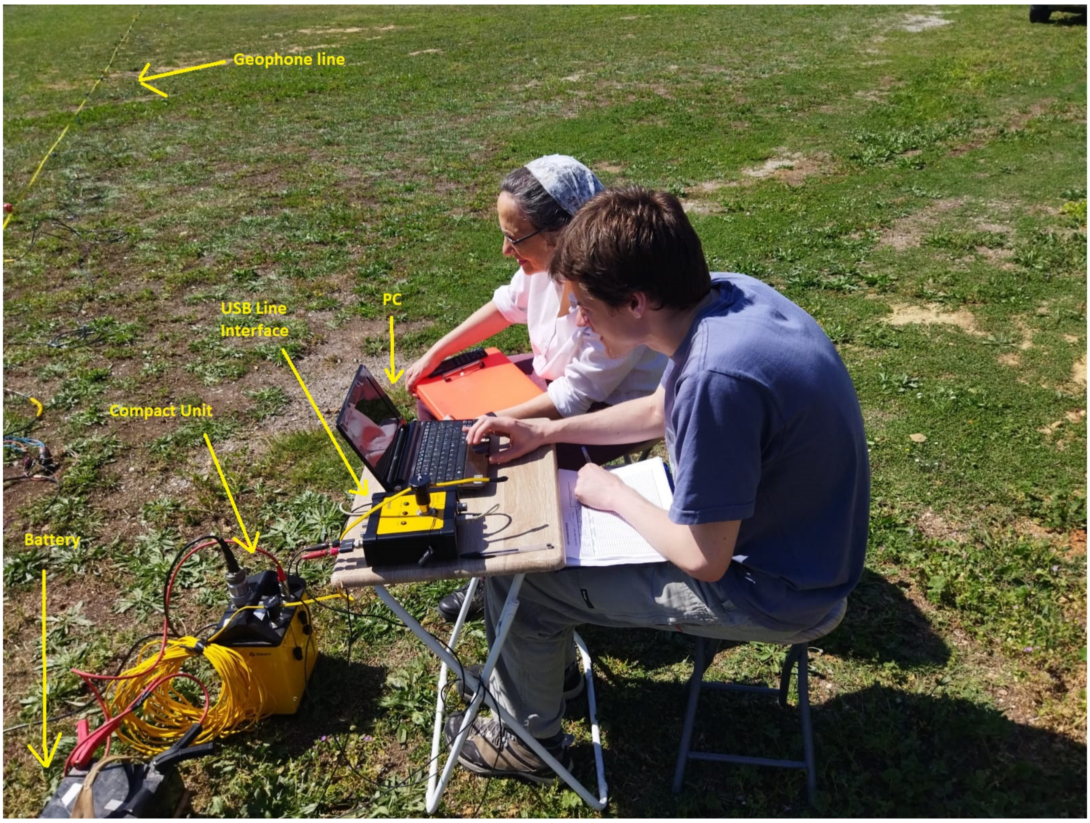

FIG. Appx.2: Checking the register obtained. Sight to the acquisition equipment and PC (day 2).

B. Software interface and outputs

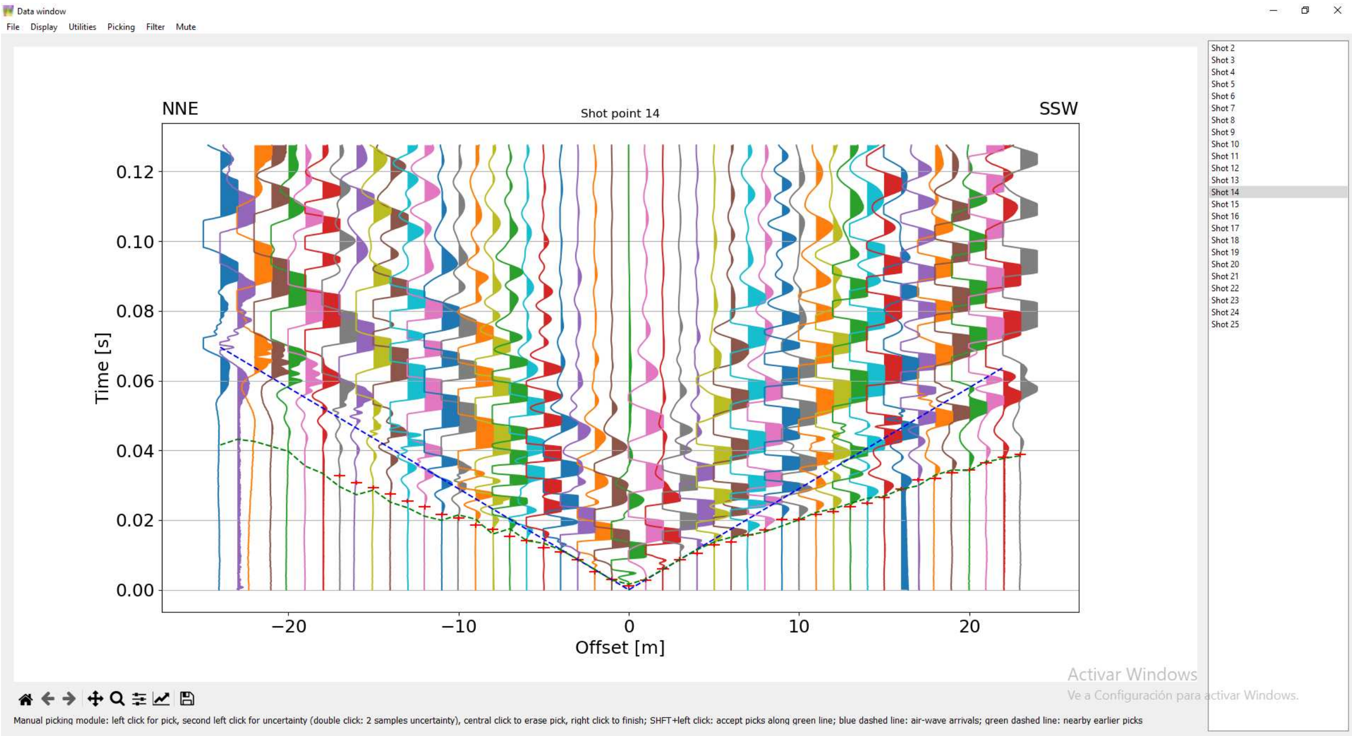

FIG. Appx.3: Example of the interface of the PyRefra program showing a good shot. The x-axis represents the distance of each geophone from the wave source (Offset). The red crosses are the picked points. The blue lines are the aerial (direct) wave arrivals. The green lines are an estimate of the first arrivals suggested by the program after the first good shot has been picked.

GeoCheck1: Bloc de notas

Archivo Edición Formato Ver Ayuda

```
**********************************************************************
*************   SUMMIT Geophone Check   06 Mar 2024   12:16:35   *************
**********************************************************************

  No  Line  Stat      Unit Impedance  Damping  Leakage  NatFreq  Noise
                               [Ohm]      [%]              [Hz]   [mV]

   1     0     0  174-   11   301.355       43      Yes       10  0.038
   2     0     0  174-   12   312.606       43      Yes       10  0.015
   3     0     0  174-   21   303.668       44      Yes       10  0.022
   4     0     0  174-   22   305.974       43      Yes       10  0.028
   5     0     0  174-   31   349.803       43      Yes       10  0.055
   6     0     0  174-   32    362.51       45      Yes       10  0.028
   7     0     0  174-   41   295.027       45      Yes       10  0.020
   8     0     0  174-   42   307.062       45      Yes       10  0.019
   9     0     0  174-   51   303.803       43      Yes       10  0.023
```

FIG. Appx.4: Partial image of the geophone check performed the first day of tests.

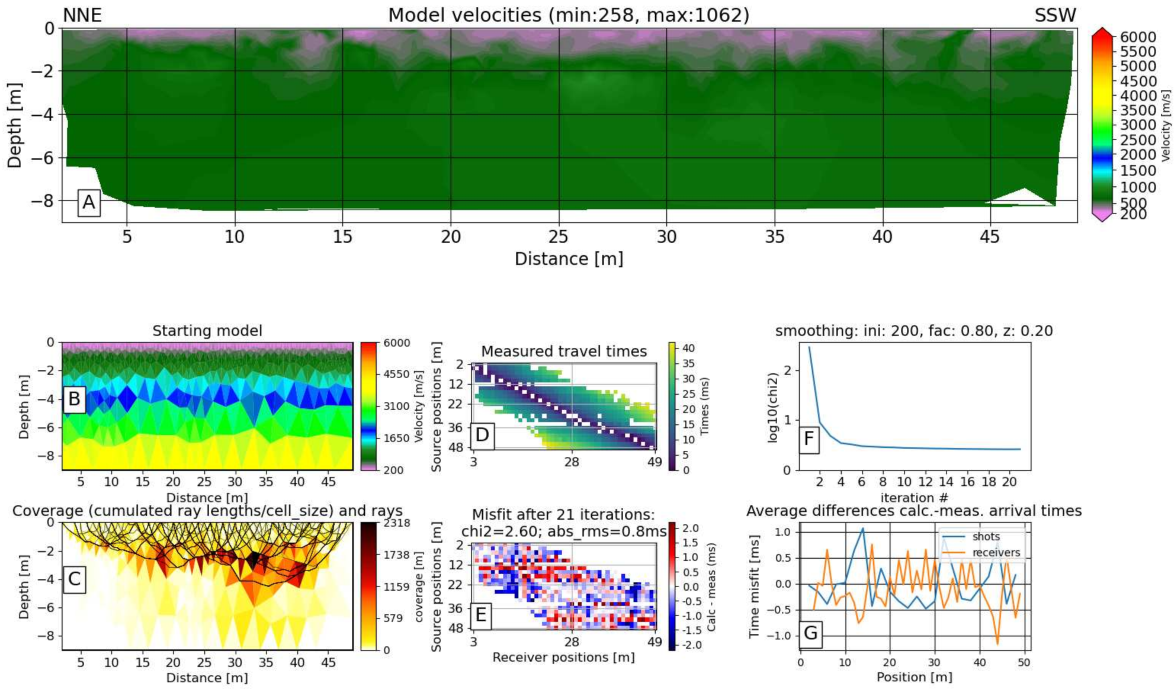

FIG. Appx.5: Complete final result output after inversion with PyRefra. Note that, in graph **C**, the ray traces calculated show the real depth simulated so, for a depth lower than 4m, the resulting model is not reliable. In graphs **E** and **G** is represented the discrepancy between the final model and the picking data. As this misfit is pretty homogeneous, we may assume that our picking is acceptable and that there is not a heavy impact from the lateral boundary effects of modelling a 3D space as it was an ideal 2D surface.

C. Description of the input files

To help with the management of the signal SG2 files produced by the acquisition equipment, the PyRefra program uses 3 support input files: "shots.geo", which locates each shot in its spacial coordinates; "receivers.geo", which locates each receiver in its spacial coordinates (the geometry of our setup); and the "file_corrections.dat", which links each SG2 file with the corresponding shot and receivers and allows modifications to the raw data. This last file is the one used to correct the delay or pre-trigger times.

The correct assemble of these files has allowed us to merge, for every shot point, the two data files we have with 24 receivers, before and after the geophone displacement, into a single large shot with 48 registers.

receivers: Bloc de notas

Archivo Edición Formato Ver Ayuda

1	2.00	0	0
2	3.00	0	0
3	4.00	0	0
4	5.00	0	0
5	6.00	0	0
6	7.00	0	0
7	8.00	0	0
8	9.00	0	0
9	10.00	0	0
10	11.00	0	0
11	12.00	0	0
12	13.00	0	0
13	14.00	0	0
14	15.00	0	0
15	16.00	0	0
16	17.00	0	0

shots: Bloc de notas

Archivo Edición Formato Ver Ayuda

1	1.00	0	0
2	2.00	0	0
3	4.00	0	0
4	6.00	0	0
5	8.00	0	0
6	10.00	0	0
7	12.00	0	0
8	14.00	0	0
9	16.00	0	0
10	18.00	0	0
11	20.00	0	0
12	22.00	0	0
13	24.00	0	0
14	26.00	0	0
15	28.00	0	0

file_corrections: Bloc de notas

Archivo Edición Formato Ver Ayuda

1	1	1	2	0.	1
2	2	1	2	0.	1
3	3	1	2	0.	1
4	4	1	2	0.	1
5	5	1	2	0.	1
6	6	1	2	0.	1
7	7	1	2	0.	1
8	8	1	2	0.	1
9	9	1	2	0.	1
10	10	1	2	0.	1
11	11	1	2	0.	1
12	12	1	2	0.	1
13	13	1	2	0.	1
14	14	1	2	0.	1
15	15	1	2	0.	1
16	16	1	2	0.	1
17	17	1	2	0.	1

FIG. Appx.6: Caption of the input files needed to run the PyRefra software. Column labels are the following. 1, "receivers.geo": Receiver number, x position (m), y position (m) , z position (m). 2, "shots.geo": Shot point number, x position (m), y position (m) , z position (m). 3, "file_corrections.geo": File number, Shot point number, first receiver number, step in receiver number, trigger time correction, interpolation factor.